*land*

MDPI

*Article*

# Integration between Dockless Bike-Sharing and Buses: The Effect of Urban Road Network Characteristics

**Zhaowei Yin [1], Yuanyuan Guo [2], Mengshu Zhou [1,*], Yixuan Wang [1,*] and Fengliang Tang [1]**

[1] School of Architecture, Tianjin University, Tianjin 300072, China; yzw1983@tju.edu.cn (Z.Y.); tang_fengliang@tju.edu.cn (F.T.)
[2] School of Architecture and Urban Planning, Guangzhou University, Guangzhou 510006, China; yuanyuanguo@gzhu.edu.cn
* Correspondence: zhoumengshu@tju.edu.cn (M.Z.); simoneinthepool@tju.edu.cn (Y.W.)

**Abstract:** Globally, dockless bike-sharing (DBS) systems are acclaimed for their convenience and seamless integration with public transportation, such as buses and metros. While much research has focused on the connection between the built environment and the metro–DBS integration, the influence of urban road characteristics on DBS and bus integration remains underexplored. This study defined the parking area of DBS around bus stops by a rectangular buffer so as to extract the DBS–bus integration, followed by measuring the access and egress integration using real-time data on dockless bike locations. This indicated that the average trip distance for DBS–bus access and egress integration corresponded to 1028.47 m and 1052.33 m, respectively. A zero-inflated negative binomial (ZINB) regression model assessed how urban roads and other transportation facilities correlate with DBS–bus integration across various scenarios. The findings revealed that certain street patterns strongly correlate with frequent connection hotspots. Furthermore, high-grade roads and 'dense loops on a stick' street types may negatively influence DBS–bus integration. The increase in the proportion of three-legged intersections and culs-de-sac in the catchment makes it difficult for bus passengers to transfer by DBS. These insights offer valuable guidance for enhancing feeder services in public transit systems.

**Keywords:** dockless bike-sharing (DBS); bus; road network characteristics; street pattern; Tianjin

check for updates

**Citation:** Yin, Z.; Guo, Y.; Zhou, M.; Wang, Y.; Tang, F. Integration between Dockless Bike-Sharing and Buses: The Effect of Urban Road Network Characteristics. *Land* **2024**, *13*, 1209. https://doi.org/10.3390/land13081209

Academic Editor: Bindong Sun

Received: 5 July 2024
Revised: 28 July 2024
Accepted: 1 August 2024
Published: 5 August 2024

**Copyright:** © 2024 by the authors. Licensee MDPI, Basel, Switzerland. This article is an open access article distributed under the terms and conditions of the Creative Commons Attribution (CC BY) license (https://creativecommons.org/licenses/by/4.0/).

## 1. Introduction

In response to the global climate crisis, international bodies, such as the 6th Intergovernmental Panel on Climate Change (IPCC), have emphasized the urgent need for comprehensive strategies to reduce emissions in the transportation sector [1,2]. A significant approach for achieving low-carbon transportation involves enhancing integrated transport services. Particularly, the integration of shared mobility services, such as dockless bike-sharing (DBS) with public transport, offers substantial benefits for urban transportation efficiency and sustainability. This multimodal integration addresses critical urban challenges, including congestion and air pollution, while increasing the competitiveness of the transportation system by offering more reliable and diverse travel options. Notably, the flexibility of DBS systems, which do not require docking stations, allows users to access bike-sharing services more freely, thereby enhancing the connectivity of public transportation networks over traditional docked bikes [3,4]. This has contributed to the global proliferation of bike-sharing programs, with over 1750 active and 265 upcoming projects across approximately 2000 cities as of September 2021 [5].

Recent research has increasingly focused on the integration of DBS with public transport, examining the role of proximity to transport stations as a key factor influencing DBS usage [6,7]. Studies have consistently shown a high frequency of DBS use near public transport stations, indicating effective integration [8]. Additionally, research has explored DBS integration with metro systems through GPS location data analysis [9] and the impact

of the built environment on this integration [10,11]. However, the integration between DBS and buses has not been as thoroughly examined. Compared to DBS–metro integration, the temporal and spatial characteristics of DBS–bus integration are less understood, and the relationship between DBS–bus integration and urban road configurations has not been explicitly discussed. These research gaps highlight the critical needs to comprehend how DBS can effectively complement bus services, as well as the further suggestions for areas where buses constitute a fundamental component of public transport.

This paper aims to fill these gaps by studying the integration of shared bikes with bus services in Tianjin, exploring how urban road configurations may influence this integration. It endeavors to address the following questions: (1) What are the temporal and spatial dynamic features of DBS–bus integration across different time periods? (2) What are the characteristics of urban road network and street patterns for cycling integrated with bus services in Tianjin? (3) Is there any correlation between this integration usage and road network characteristics? The findings are intended to support the design of seamless connections between DBS and public buses, emphasizing improvements in infrastructure and policies that promote cycling-friendly environments and green urban mobility.

The remainder of this paper is organized as follows: Section 2 reviews the literature on the integration of bikeshare systems and public transport as well as the impact of urban roads on the integration. Section 3 describes the study area, data collection, measurement of the integrated usage, and statistic models applied. Section 4 presents the empirical findings and critical analysis, in detail. Finally, Section 5 concludes the paper with policy recommendations, practical implications, and research limitations.

## 2. Literature Review

### *2.1. Integration of Bikeshare and Public Transport*

The integration between bike-sharing and public transport mainly occurs through two pathways: access (cycling to the station) and egress (cycling from the station). DBS systems, unlike docked systems, allow for parking near transit stations, which enhances flexibility and efficiency. The lack of docking constraints enables a closer integration with public transport systems compared to their docked counterparts [10].

Most existing studies have predominantly focused on quantifying the integration of shared bicycles and metro stations, paying less attention to their integration with bus services. The presence or absence of docking systems plays a crucial role in measuring integration behaviors. Docked systems often use a unified card system that facilitates the use of a single transport card for both public transit and bike usage, making it easier to track integration [12–14]. Thus, a traditional method to identify bikeshare–metro trips is to analyze the smart card data that combine the records of bike-sharing and metro transactions. However, this approach is not applicable to DBS, which relies on smartphone applications rather than smart cards [12,15]. Furthermore, the common walking distances between DBS bicycles' starting/ending points and bus stations are largely undocumented, which complicates the accuracy of integration measurements.

Due to the lack of docking systems, DBS–metro integration is identified by establishing buffer zones around metro stations, typically 50 m or 100 m buffers [16–18]. To more precisely identify the most feasible parking area around a metro station, a further delineation, known as a "parking ring", considering the possibility of locking and unlocking behavior, is established on the buffer [11]. Integrated usage is often gauged by the frequency of DBS usage within the parking areas of metro stations [19]. Additionally, scholars have also considered the constraints of passenger volume at the metro station level to refine the measurement of integration behaviors [14].

Conversely, the integration of shared bicycles with buses shows distinct characteristics. Bus stations, typically smaller and less complex than metro stations, attract fewer integrated users. Furthermore, unlike metro stations, which may have multiple entrances spaced apart, bus stops are more uniformly distributed along roadsides, affecting the methods

used to measure integration. Nonetheless, research on bike–bus integration is limited and often adapts methodologies from studies focused on metro stations [18].

### *2.2. Urban Road Network Influencing the Integration of Bikeshare and Public Transport*

#### 2.2.1. Analysis of Road Network Characteristics in the Context of Built Environment Effects

Transportation infrastructure plays a pivotal role in the integration of shared bicycles with public transportation. The street network, characterized by its topological configuration and connectivity [20], is a crucial component of the built environment. It profoundly influences how individuals interact with their surroundings and participate in various activities [21,22]. Some studies have found that high-density road networks positively impact the ridership of shared bicycles [23]. Additionally, road intersection density has shown varying correlations with bike-and-ride trips in different cities: it positively correlates in Beijing but negatively in Taipei and Tokyo [24]. Conversely, high traffic volumes and potential congestion on major roads may hinder bike-and-ride integration [8,15].

These studies, however, often lack a detailed analysis of road structure patterns and characteristics, relying instead on common metrics, such as road density and intersection number. This approach leads to significant variability in findings between study areas and less targeted conclusions. Moreover, these studies predominantly focus on metro connections, with limited exploration of how road structures impact the integration of shared bicycles with bus stations.

#### 2.2.2. Quantifying Road Characteristics in Studies Related to Shared Bicycle Riding Behavior

Cycling behaviors are influenced by various levels of urban roads, from pedestrian spaces to urban motor lanes. Therefore, it is essential to highlight the importance of urban road traffic network characteristics [25].

Many studies introduce graph theory to simplify road structures into graph structures composed of nodes (road intersections) and edges (road segments). By computing various complex topological metrics, researchers uncover road characteristics related to connectivity and accessibility, including but not limited to network centrality [26,27], the meshedness coefficient [28–30], and the average geodesic distance [26,31]. However, these studies, while useful, often focus on collision data to analyze the impact of road morphology on cycling safety, with less attention given to connectivity with buses.

Based on this framework, numerous studies classify neighborhoods into various road configurations and patterns using one or more topological metrics. These patterns, while often resembling each other, encompass several common predefined structural types: gridiron, parallel, loops and lollipops, mixed, and others [26,27]. They have increasingly been employed in urban cycling research due to their impact on cycling behaviors, such as traffic flow distribution [26,32]. Some argue that the gridiron pattern offers better cycling connectivity compared to other layouts [33].

However, it is important to note that the influence of road configurations on cycling behaviors cannot be universally generalized, as conclusions vary across different time periods. Additionally, the spatial scale of distances within urban environments also significantly influences cycling behaviors. Moreover, while integration with public transport is crucial, it remains an underexplored area of study. Thus, incorporating both spatial configurations and varying timeframes is essential for accurately reflecting and analyzing the real demands for integrating shared bicycles with public transport systems.

### *2.3. Other Factors Influencing the Integration of Bikeshare and Public Transport*

Transfer distance critically impacts the integration of bicycles with public transport. The distance between stations and homes or workplaces heavily influences the choice of feeder modes, with most passengers opting for DBS when the transfer distance exceeds 800 m [17,24]. Interestingly, trips originating from home tend to tolerate longer distances compared to those from workplaces [17,34]. Considering that bus systems typically

involve longer waiting times, the acceptable threshold distance for cycling might be shorter compared to that for metros, reflecting a lower tolerance for time costs associated with bus transfers [35].

Urban land use correlates with urban density and human activities, affecting the feeder mode choices of public transport. Specific land use types, such as residential, industrial, and educational, have been positively associated with increased bike and metro integration. Notably, the presence of green spaces enhances the likelihood of cycling to metro stations by providing a conducive cycling environment away from traffic and potential hazards [11,36]. In bus usage, various land use types promote DBS and public transport integration, but high-density commercial areas may deter cyclists due to pedestrian congestion [37]. Mixed land use positively impacts bike trips to and from metro stations in cities such as Melbourne, Toronto, and Taipei, though it shows a negative association with egress use for DBS [24,38,39].

Well-maintained bicycle infrastructure, such as dedicated lanes and secure parking, is crucial for facilitating access to metro stations [40–42]. In addition, integration patterns vary geographically, being more prevalent in inner suburbs of North American cities and in city centers or subcenters in Asian cities, such as Beijing [43]. Some studies, however, indicate no significant difference in integrated use between core and peripheral areas [11,44].

## 3. Method

### *3.1. Study Area*

Tianjin, located in the northern region of China, is one of the four municipalities directly under the central government of China. As of 2022, it has a permanent population of approximately 13.866 million and spans an area of about 11,946 km$^2$. The city is divided into 16 districts: 6 urban, 4 suburban, and 5 exurban counties, and the Binhai New Area. The urban districts, which host the majority of the city's public facilities, are densely populated and have a well-developed transportation infrastructure. This study focuses on these six urban districts, where the demand for integrated public transportation is particularly high (Figure 1).




**Figure 1.** Study area of Tianjin and the distribution of bus stops.

Tianjin's public bus system constitutes a vital component of its public transportation network. By the end of 2023, the system included 693 bus routes covering 15,797 km,

serviced by 6412 vehicles. Bus stations are distributed extensively throughout the central urban area, ensuring 100% coverage within a 500 m radius. In 2023, the buses handled approximately 472.66 million passenger trips, accounting for 27% of the total public transportation passenger flow. Furthermore, to promote multimodal transportation, the government has implemented economic incentives, such as fare discounts for transfers between buses within a two-hour window and between buses and rail transit.

### *3.2. Data*

In this study, data on the starting points of dockless bike-sharing were used to identify the integration of cycling with buses. The data were obtained from the Tianjin Municipal Transportation Commission. These data included operational information from three companies: HelloBike, Meituan Bike, and Qingju, which represent all shared bicycle operators in Tianjin. All datasets contain vehicle IDs, start and end locations (longitude and latitude accurate to six decimal places), and start times (accurate to the second).

Data were collected over seven days from 18 September to 24 September 2023. During this period, the average temperature ranged between 18.4 °C and 26.7 °C, and the weather conditions were favorable for cycling travel, including both sunny and cloudy conditions. Approximately 190,157 records of bicycle trips were gathered, providing a comprehensive view of cycling activity in Tianjin.

The inclusion of both weekdays and weekends in the data collection helped to capture the variability in intermodal behavior throughout the week. Additionally, analyzing the continuous weekday and weekend data was expected to address potential day-to-day variances. Empirical studies suggest that the patterns of dockless bike-sharing usage are consistent across weekdays [11,45], supporting the assumption that the selected week is representative of typical weekly usage.

Furthermore, information about the bus stations, including the names and coordinates, was sourced from Baidu Maps (http://api.map.baidu.com/ (accessed on 15 September 2023)), which is a reliable open data source in China. Road information was obtained from OpenStreetMap (https://www.openstreetmap.org/ (accessed on 8 June 2023)), covering the entirety of Tianjin city. This comprehensive dataset facilitated a detailed analysis of the integration between dockless bike-sharing and the bus network within the urban districts of Tianjin.

### *3.3. Measuring the Variables*

#### 3.3.1. Measure of the DBS–Bus Integrated Use

Previous research primarily quantifies integration with metro stations, typically using a 50 m or 100 m buffer to define parking areas. In contrast, due to their smaller size and proximity to roads, bus stations might lead to overestimations of transfer frequency using traditional buffers. For this study, a rectangular buffer of 100 m in length and 10 m in width, centered on the bus stops, delineated the probable parking area. In line with Guo et al. [15], the use of other modes of transportation for bus access and egress was measured by the effective usage count within the parking area.

The integrated usage was identified in the following four steps (Figure 2): (1) processing the raw data, (2) calculating the orientation of the parking areas, (3) establishing the parking area, and (4) distinguishing the access and egress integrated usage.

Step 1: Processing the raw data

For subsequent calculations, processing the raw data was essential. Since road distances are often long and not necessarily straight, it was necessary to clip the roads to better determine the orientation of the parking areas. Therefore, after intersecting line breaks of the road shapefile, a 50 m circular buffer was established around the bus stops to clip the roads. Subsequently, each clipped road segment was geocoded in the GIS.

Additionally, in the raw data of trip records, there were instances of missing coordinates and inconsistent coordinate units among different modes of transportation. Therefore, the data were cleaned to extract valid starting and ending point coordinates.

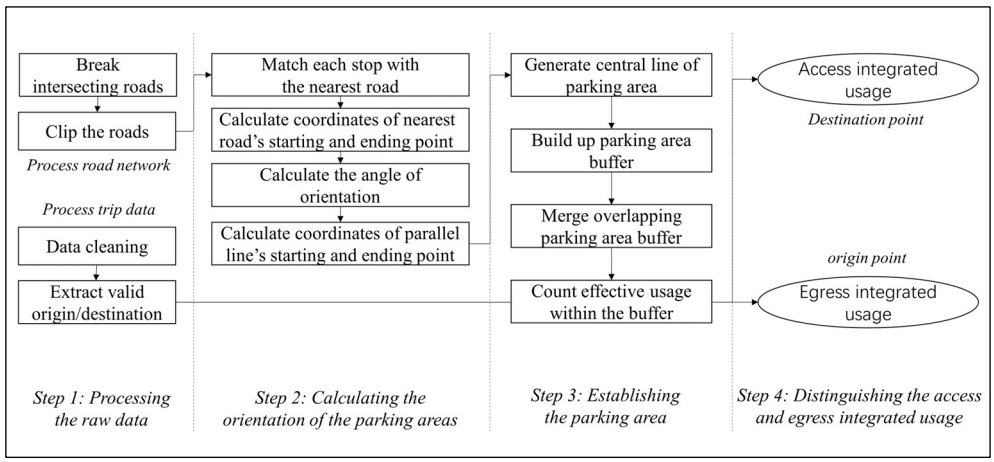


**Figure 2.** Complete process of identifying the integrated usage.

Step 2: Calculating the orientation of the parking areas

To determine the orientation of the transfer area based on the surrounding road environment, we used the road as a directional reference to determine the coordinates of the endpoints of the central line of the transfer area.

Each bus stop was initially geocoded in the GIS. GIS generated a near table to match each stop with the nearest road. As shown in Figure 3a, for each stop, O ($X$, $Y$), the coordinates of the nearest road's starting point, A ($X1$, $Y1$), and ending point, B ($X2$, $Y2$), were calculated. Based on this information, the angle of orientation of the road was calculated using the following formula:

$$angle = \tan((Y2 - Y1)/(X2 - X1)) \times (180/\pi) \quad (1)$$

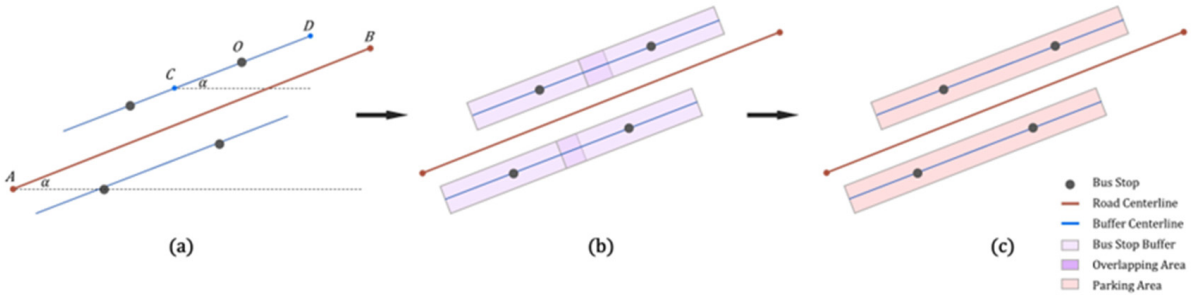


**Figure 3.** Diagram of the process for establishing parking areas, including determining the direction of the buffer zone (**a**), determining the size of the buffer zone (**b**), and merging overlapping areas (**c**). In (**a**), letters AB represent two points on the centerline of the road, CD are the two endpoints of the generated buffer zone centerline segment, and O denotes the bus stop.

To calculate the coordinates of the starting point, C ($X3$, $Y3$), and ending point, D ($X4$, $Y4$), of the parallel line passing through the corresponding stop:

$$\begin{cases} X3 = X + distance/2 \times \cos(angle) \\ Y3 = Y + distance/2 \times \sin(angle) \\ X4 = X - distance/2 \times \cos(angle) \\ Y4 = Y - distance/2 \times \sin(angle) \end{cases} \quad (2)$$

In this context, distance refers to the length of the buffer zone, which was set at 100 m.

Step 3: Establishing the parking area

After connecting each pair of starting points obtained in the previous step, the central line of each parking area was obtained. Then, as shown in Figure 3b, a 5 m buffer was generated for each line, resulting in parking areas with a length of 100 m and a width

of 10 m. It is worth noting that in real-life scenarios, some bus stops have multiple bus routes passing through them. Therefore, multiple stations may be set up in areas nearby, leading to overlapping parking areas for such stations. To avoid duplicated calculations, we merged these overlapping parking areas into one. Then, the geometric center of the merged catchment areas was extracted to represent the adjacent stations and, finally, a total of 1719 bus integration stops were obtained within the 6 districts of the city.

Step 4: Distinguishing the access and egress integrated usage

In general, the integrated usage of other transport modes and buses can be identified in two modes—(1) access integrated usage: the trip with a destination located in the parking area, and (2) egress integrated usage: the trip with an origin located in the parking area. Total integrated usage should comprise both access and egress integrated usage.

This assumes that users of DBS who drop off within a certain space near bus stops have the purpose of taking the bus, while travelers who pick up a bike in close proximity to bus stops have already finished their bus trips. This assumption was also similarly raised by Wu et al. [22] and Guo and He [11].

In order to thoroughly explore the impact of road characteristics on DBS–bus integrated usage, we divided the typical traffic flow into three time periods, namely, the peak hours on weekdays, the off-peak period on weekdays, and the weekend. It was matched to access integration, egress integration, and total integration to form a total of 3*3 usage scenarios, which were then input into the model as dependent variables. Their frequency statistics are shown in Table 1.

**Table 1.** Integration frequency statistics of nine dependent variables.

| Dependent Variables | Mean | Std. | Min. | Max. |
|---|---|---|---|---|
| Access integrated use during weekday peak hours | 3.209 | 13.215 | 0 | 401 |
| Egress integrated use during weekday peak hours | 3.274 | 10.654 | 0 | 200 |
| Total integrated use during weekday peak hours | 6.483 | 22.952 | 0 | 598 |
| Access integrated use during weekday off-peak hours | 4.383 | 12.924 | 0 | 347 |
| Egress integrated use during weekday off-peak hours | 4.342 | 10.485 | 0 | 178 |
| Total integrated use during weekday off-peak hours | 8.724 | 22.596 | 0 | 525 |
| Access integrated use during weekend | 5.857 | 17.903 | 0 | 506 |
| Egress integrated use during weekend | 5.873 | 14.108 | 0 | 270 |
| Total integrated use during weekend | 11.729 | 31.145 | 0 | 776 |

#### 3.3.2. Measure of Urban Road Network Variables and Control Variables

The catchment area radiating around each bus stop served as the unit for measuring all independent variables. Considering the average DBS–bus trip distances (1028.47 m for access and 1052.33 m for egress), a 1000 m search radius was selected to assess urban road attributes around bus stops. In accordance with existing research, the explanatory variables in this study were categorized into road features in size and road network structure features. Using OpenStreetMap data, roads were simplified and transformed into an unweighted, undirected line graph, where roads and intersections became nodes and edges, respectively. Based on this, we calculated the density of roads in the catchment area of each bus stop, including major roads, secondary roads, branch roads, and residential roads [11,46,47]. The number and proportion of different intersections were also calculated. The grade of the nearest road was assigned to each bus stop as a classification variable, namely, whether the bus stop is along the major roads, secondary roads, branch roads, or residential roads was identified.

In addition to these common features, the centrality of road networks was also analyzed based on topology and graph theory. It is an index to measure the importance of nodes in the network. Zhang et al. [48] and Li et al. [27] observed that betweenness centrality and eigenvector centrality performed better than degree centrality and closeness centrality for distinguishing road network patterns. In this study, we used network betweenness centrality, which is based on point betweenness centralities, to describe the

degree of independence between nodes in a road network [28,31,49]. Point betweenness centrality is calculated by:

$$C_k^B = \sum_{i,j \in N, i \neq j \neq k} \frac{n_{ij}(k)}{n_{ij}} \quad (3)$$

where $n_{ij}$ is the total number of shortest paths from node $i$ to node $j$, $n_{ij}(k)$ is the number of shortest paths between node $i$ and node $j$ that contain node $k$, and $N$ denotes the total number of vertices in the network.

In the road network, via the dual approach, greater point betweenness centrality means the road is more important in connecting road pairs. The calculation quotation for network betweenness centrality in each catchment is as follows:

$$C^B = \frac{\sum_{k=1}^{n} \left(C_{k^*}^B - C_k^B\right)}{\max\left(\sum_{k=1}^{n} \left(C_{k^*}^B - C_k^B\right)\right)} \quad (4)$$

where $C_{k^*}^B$ is the maximum betweenness centrality value for all nodes in a catchment area, $\sum_{k=1}^{N} \left(C_{k^*}^B - C_k^B\right)$ is the sum of the differences between the maximum value and each node $k$, and max $\left(\sum_{k=1}^{n} \left(C_{k^*}^B - C_k^B\right)\right)$ means the possible maximum sum of these differences.

A higher value of network betweenness centrality indicates that there is a greater difference in point betweenness centrality among all individual roads. Typically, the lollipop and cul-de-sac networks tend to have higher network betweenness centrality than other street patterns, showing lower inter-connectivity and accessibility [50].

The eigenvector centrality suggests that a node is more central, as it is connected to important nodes [51]. A node with high eigenvector centrality is not surely well connected to others. It is calculated as follows:

$$x_v = \frac{1}{\lambda} \sum_{t \in M(v)} x_t \quad (5)$$

where $x_v$ is the eigenvector centrality of node $v$, $\lambda$ is a constant, and $M(v)$ represents the adjacency matrix of node $v$. The network eigenvector centrality of each catchment is the average value of that of all the nodes within.

In order to further explore the influence of road network structure features on integrated usage, the hierarchical clustering method was used to derive the morphometric-based street patterns from several metrics generated previously. Then, the categorized street pattern also became one of the explanatory variables for modeling. Hierarchical clustering is a machine learning technique for grouping data points into classes of similar objects. Three indicators, network betweenness centrality, road density, and number of intersections, were jointly introduced for the hierarchical clustering. The distance function used included complete linkage, average linkage, and ward.

The ideal method and number of clusters in this study was determined by comparing the silhouette score, which measures how similar an object is to its own cluster compared to other clusters. Based on the final clustering results, the main factors' average value and the mean of the sum of squares corresponding to each category were calculated to determine the characteristics of various street patterns.

In addition, land use indicators and public transport facilities were also included as control variables. Five categories of Points of Interest (POIs) were used to measure land use patterns: residence, companies, education facilities, restaurants, and shops. Using POI data to estimate land use might be preferable because it might perform better to describe the land use than via land cover maps [52–54]. As for transport facilities, we took into account the distance to the nearest metro stations of each bus stop since DBS could potentially integrate with the nearby metro systems. Additionally, we gauged the distance from bus stations to the CBD to characterize the metro station's location. Transfer distance represents the average driving distance in three scenarios during three time periods and had a great

influence on the actual integration frequency. Descriptive statistics of the variables are shown in Table 2.

**Table 2.** Definition and descriptive analysis of the variables (N = 1719).

| Variables | Description | Mean | Std. | Min. | Max. |
|---|---|---|---|---|---|
| **Road features in size** | | | | | |
| Road grade | The grade of the road along which the bus stop is located | 2.226 | 0.967 | 1 | 4 |
| Road density | Total road length divided by area in square kilometers (km/km$^2$) | 6.697 | 2.048 | 2.531 | 15.255 |
| Major road density | Arterial density in the catchment area (km/km$^2$) | 0.922 | 0.516 | 0 | 2.262 |
| Secondary road density | Density of the secondary road (km/km$^2$) | 1.196 | 0.663 | 0 | 3.720 |
| Branch road density | Collector road density in the area (km/km$^2$) | 1.628 | 0.975 | 0 | 6.325 |
| Residential road density | Density of residential road in each area (km/km$^2$) | 2.951 | 1.889 | 0.086 | 11.950 |
| **Road network structure features** | | | | | |
| Betweenness centrality | The degree of independence between nodes in the network | 0.398 | 0.214 | 0.028 | 1.000 |
| Eigenvector centrality | The average value of nodes' eigenvector centrality in the network | 0.268 | 0.052 | 0.144 | 0.437 |
| Number of intersections | Number of street intersections in the catchment area | 57.198 | 38.630 | 11 | 268 |
| Number of 3-legged intersections | Number of 3-legged intersections in the catchment area | 32.645 | 19.608 | 6 | 140 |
| Proportion of 3-legged intersections | The proportion of 3-legged intersections in the catchment area | 0.589 | 0.090 | 0.300 | 0.923 |
| Number of 4-legged intersections | Number of 4-legged intersections in the catchment area | 20.867 | 18.923 | 1 | 122 |
| Proportion of 4-legged intersections | The proportion of 4-legged intersections in the catchment area | 0.338 | 0.102 | 0.071 | 0.632 |
| Number of culs-de-sac | Number of culs-de-sac in the catchment area | 3.129 | 2.391 | 0 | 11 |
| Proportion of culs-de-sac | The proportion of culs-de-sac in the catchment area | 0.066 | 0.062 | 0 | 0.333 |
| **Land use (POIs)** | | | | | |
| Residential use density | Number of residential buildings | 65.084 | 36.191 | 10 | 231 |
| Company density | Number of companies and factories, etc. | 113.357 | 88.941 | 4 | 554 |
| Education facility density | Number of schools, universities, and other educational institutions | 6.544 | 4.487 | 0 | 29 |
| Restaurant density | Number of restaurants | 456.655 | 296.236 | 23 | 1964 |
| Shopping use density | Number of malls, supermarkets, and retail stores | 90.958 | 47.997 | 8 | 290 |
| **Transport facilities** | | | | | |
| Distance to nearby metro station | Distance to the nearest metro station (km) | 0.656 | 0.409 | 0.005 | 2.445 |
| Transfer distance | Average cycling distance of integrated use in each scenario (km) | 3.207 | 0.387 | 0.371 | 4.609 |
| Distance to CBD | Distance to CBD (km) | 5.074 | 2.102 | 0.134 | 10.145 |

### *3.4. Models: Zero-Inflated Negative Binomial Regression (ZINB)*

The zero-inflated negative binomial (ZINB) regression model is a generalized linear model based on the zero inflation and the negative binomial distribution [55,56]. It is usually used to analyze countable data and address issues, such as severe skewness, excessive zero values, outliers, etc. Zero inflation refers to the presence of many zero values of the dependent variable, while negative binomial distribution means that the variance is greater than the mean. Unlike Poisson distribution, its kurtosis is much smaller, making it more suitable for modeling counting data.

Since the integration of DBS and public transport is usually counted, ZINB has been commonly applied to the research on DBS–bus integration. In the context of DBS–bus integration, where the count of DBS used as a transfer mode can often be zero, especially in areas with a dense distribution of bus stops and poor allocation of DBS bikes, the ZINB model is particularly apt. The formula of the ZINB model is presented as follows:

$$f(y|\boldsymbol{X}, p, k) = \begin{cases} p + (1-p)\left(\frac{k}{k+\mu}\right)^k, & y = 0 \\ (1-p)\frac{\boldsymbol{\Gamma}(y+k)}{\boldsymbol{\Gamma}(y+1)\boldsymbol{\Gamma}(k)}\left(\frac{k}{k+\mu}\right)^k\left(\frac{\mu}{k+\mu}\right)^y, & y > 0 \end{cases} \quad (6)$$

where $y$ is the dependent variable of DBS–bus integrated usage of three scenarios during three time periods, and $\boldsymbol{X}$ represents the independent variables of road network factors that affect the DBS–bus integration, as shown in Table 1. $\boldsymbol{\Gamma}$ is gamma distribution, and $p$ refers to the ratio of zero values of the dependent variable. $p$ can be also treated as a zero-inflated parameter, indicating that the larger the value of $p$, the more likely there is a zero-inflation phenomenon. $k$ is reciprocal of the divergence parameter, while $\mu$ is the

mean of negative nominal distribution. Additionally, the expectation and variance of the zero-inflated negative binomial distribution can be calculated as follows:

$$E(Y) = (1 - P)\,\mu \tag{7}$$

$$\mathrm{Var(Y)} = E(Y)\left[1 + \frac{\mu(1+k)}{k} - E(Y)\right] \tag{8}$$

By introducing two covariates (i.e., $\boldsymbol{X}$ and $\boldsymbol{W}$) in the zero-inflated section and negative binomial section, respectively, a complete ZINB model was established. For the dependent variable with a non-zero value, the log-linear model was applied to modeling, while the logistic model was used for modeling the dependent variable with a zero value:

$$\begin{cases} \lg(\mu) = \boldsymbol{X}^T\beta \\ logit\ (p) = \boldsymbol{W}^T\gamma \end{cases} \tag{9}$$

where $\beta$ and $\gamma$ refer to the coefficients of $\boldsymbol{X}$ and $\boldsymbol{W}$, respectively.

Nine ZINB models were developed, in accordance with the nine dependent variables. To avoid the multicollinearity problem, the variance inflation factor (VIF) of the selected explanatory variables was calculated. By following the rule of thumb, variables with VIF larger than 10 were excluded from the model.

## 4. Results and Analysis

### *4.1. Spatial and Temporal Dynamic Features of DBS–Bus Integration*

Figure 4 presents the temporal dynamics of dockless bike-sharing usage in Tianjin, where the frequency of access, egress, and total integration during eighteen hours on weekdays and weekends are shown in Figure 4a. The data revealed significant fluctuations in DBS–bus integration depending on the day and time. Notably, peak integration frequencies on weekdays occurred between 07:00 and 09:00 AM and between 17:00 and 19:00 PM. Weekends showed a broader morning peak from 07:00 to 10:00 AM, with evening peaks overlapping similarly to weekdays. During weekday mornings, integration frequencies were comparable to or exceeded those of the evening, a trend that reversed on weekends. Overall, weekend integration frequencies were about two-thirds of those on weekdays. Interestingly, egress connections during weekday peak hours tended to peak in the preceding hour compared to access connections, which is the reverse of what was observed during other times. There was also a notable midday peak in DBS–bus integration between 11:00 AM and 13:00 PM on weekdays, a pattern absent on weekends, particularly Sundays. This variation suggests differences from other large cities. For example, Li et al. [8] found that the bike use in the evening peak in Shanghai was higher than that in the morning peak, and in Nanjing, the peak of commuting time for DBS–bus integration disappeared on weekends [12]. The similarity in cycling behavior between Saturdays and weekdays, minus a significant morning peak, could indicate prevalent overtime work on weekends.

Figure 4b,c show basic statistics of bike trips of access, egress, and their average values at different times of the week, including the travelling distance and travelling time. Compared with the hourly integration frequency, these two characteristics varied more between access and egress connections. During weekday morning rush hours, the average access-cycling distance was 1498.31 m, with a travel time of 706.88 s, both shorter than those for egress, which were 1609.53 m and 812.4 s, respectively. The cycling process extended longer, to around 10:00–11:00 AM and during and after the evening rush hour, with longer access connections generally lagging behind egress connections by 2 to 3 h. In addition, travel times and distances on weekends were generally longer than those on the weekdays, without clear peak periods. These findings not only underscore the efficiency sought during fixed commuting times on weekdays but also indicate that residents are more likely to use DBS for leisurely connections between entertainment areas after work hours and on weekends. This behavioral pattern reflects a blend of utilitarian and recreational usage,

differing by time of day and week, and highlights the adaptability of DBS to varying urban mobility needs.

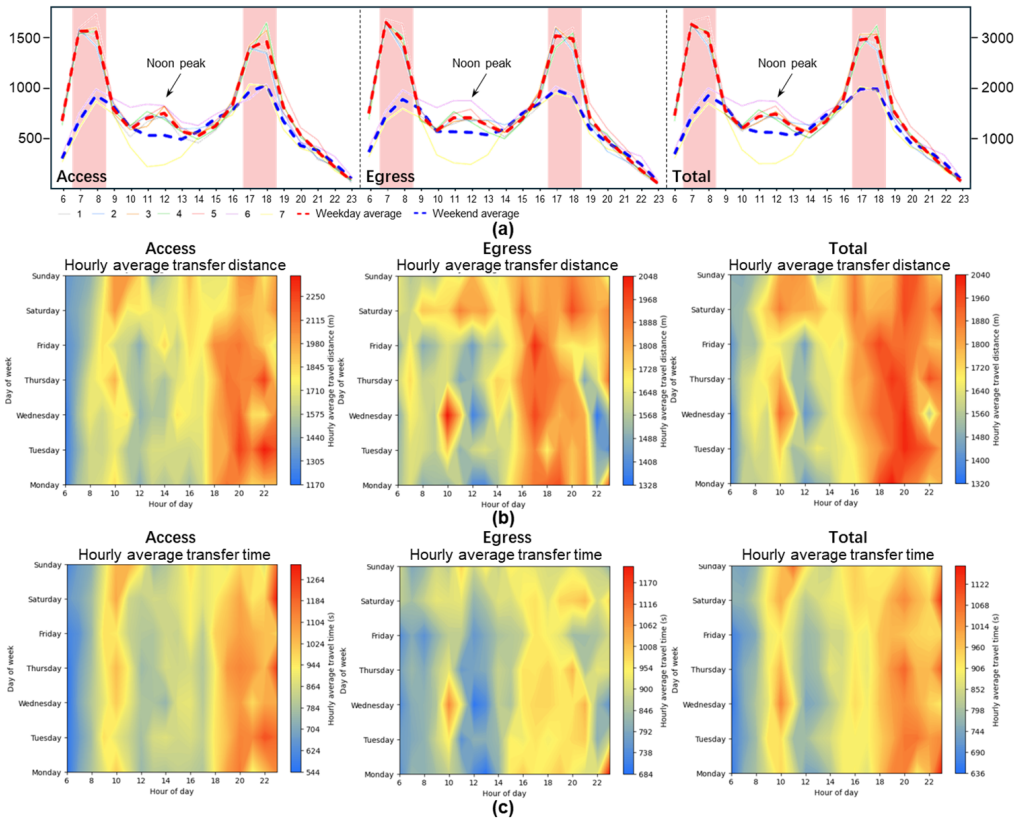


**Figure 4.** Dynamic temporal characteristics of DBS–bus integrated use in Tianjin, including the frequency of access, egress, and total integration during eighteen hours (**a**), hourly average transfer distance (**b**), and hourly average transfer time (**c**). The red lines in (**a**) represent the frequency in weekdays while the blue lines represent that at weekends.

Figure 5 shows the spatial distribution of DBS–bus integrations across three scenarios during three distinct time periods. The bus stops are uniformly distributed throughout the inner city, but notable concentrations of DBS–bus usage—where frequencies exceed zero—primarily occur in the inner city and extend along the upper and lower reaches of the Haihe River. During the weekday peak hours, the total access integration frequency in the city center and the large industrial areas in the south was significantly higher than the egress integration. This pattern suggests that DBS plays a crucial role in facilitating quick connections with public transport, especially during the commute from suburban areas to downtown. This trend was consistent, with high connection frequencies persistently localized around the old city and the commercial areas along the Haihe River. On weekends, while the high-frequency areas remained similar, there was an increase in outbound connections from the city center's commercial districts and densely populated scenic areas. This shift likely mirrors the spatial clustering of residents' recreational activities, such as shopping and entertainment, which peak over the weekend. The contrast in spatial distribution between weekdays and weekends highlights the dual role of DBS in supporting both daily commutes and leisure activities, adapting to the fluctuating urban dynamics of Tianjin.

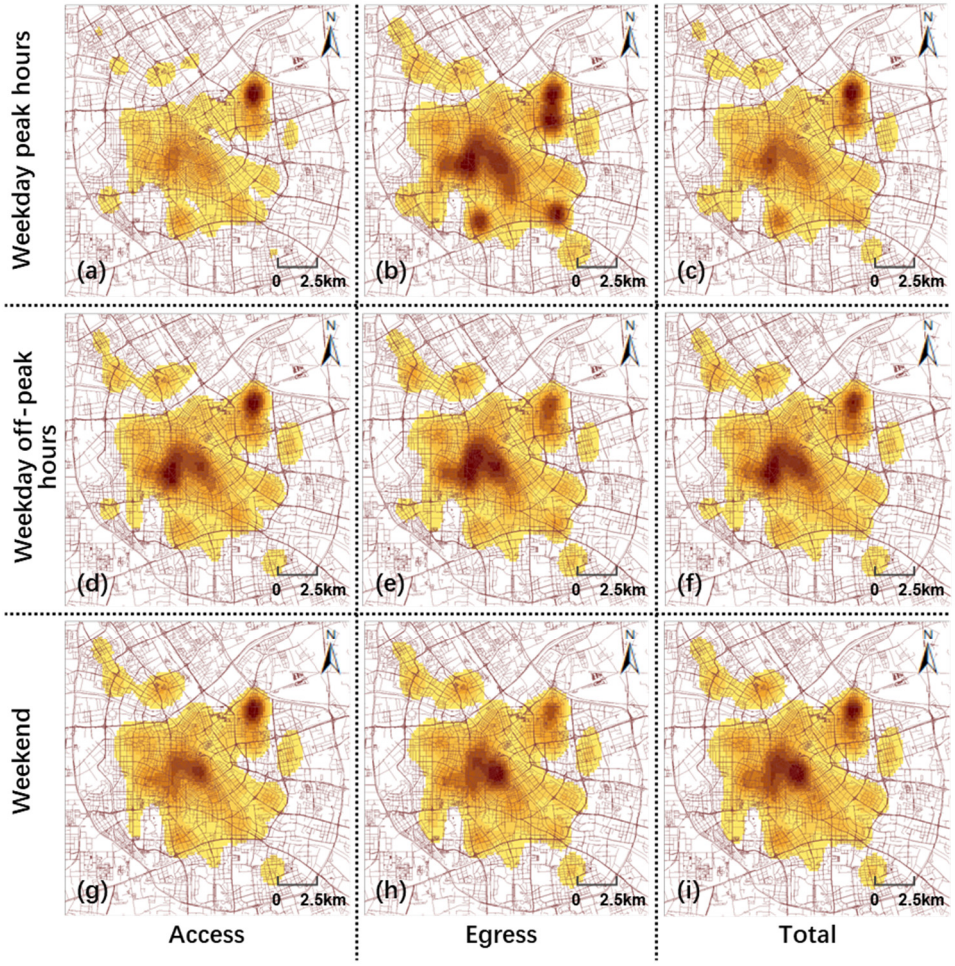


**Figure 5.** Hotspot of the access, egress, and total DBS–bus integrated use in Tianjin during weekday peak hours (**a**–**c**), weekday off-peak hours (**d**–**f**), and weekends (**g**–**i**).

### *4.2. Road Network Characteristics in Tianjin Inner City*

#### 4.2.1. Spatial Distribution Characteristics of Network Centrality

The spatial distributions of both node and network centralities in Tianjin's inner city are depicted in color-coded maps, as shown in Figure 6. Figure 6a,b show the spatial distribution of betweenness centrality, while the other two figures show eigenvector centrality. The intersection with high betweenness centrality was mainly located on the main roads, including the inner and outer ring expressway and the main road along the coastal river. These three trunk roads carry a large traffic flow and become an important connection path for urban public transportation. Accordingly, the high values of network betweenness centrality were predominantly located along the Haihe riverbanks in the city center and extended in a northwest–southeast direction. In contrast, the areas around bus stops generally exhibited lower network centralities.

The spatial distribution of eigenvector centrality of intersections exhibited a multi-core structure. High values were widely distributed in areas with more compact grid roads, including the old town business district, the fifth avenue business district, and the Zhongshan road business district. This is largely due to the better connectivity of the grid road structure. The distributions of the network eigenvector centrality were similar to that of the former, forming a high-value core in the fifth avenue business district in the city center. Areas with sparser road networks and poorer connectivity showed lower values.

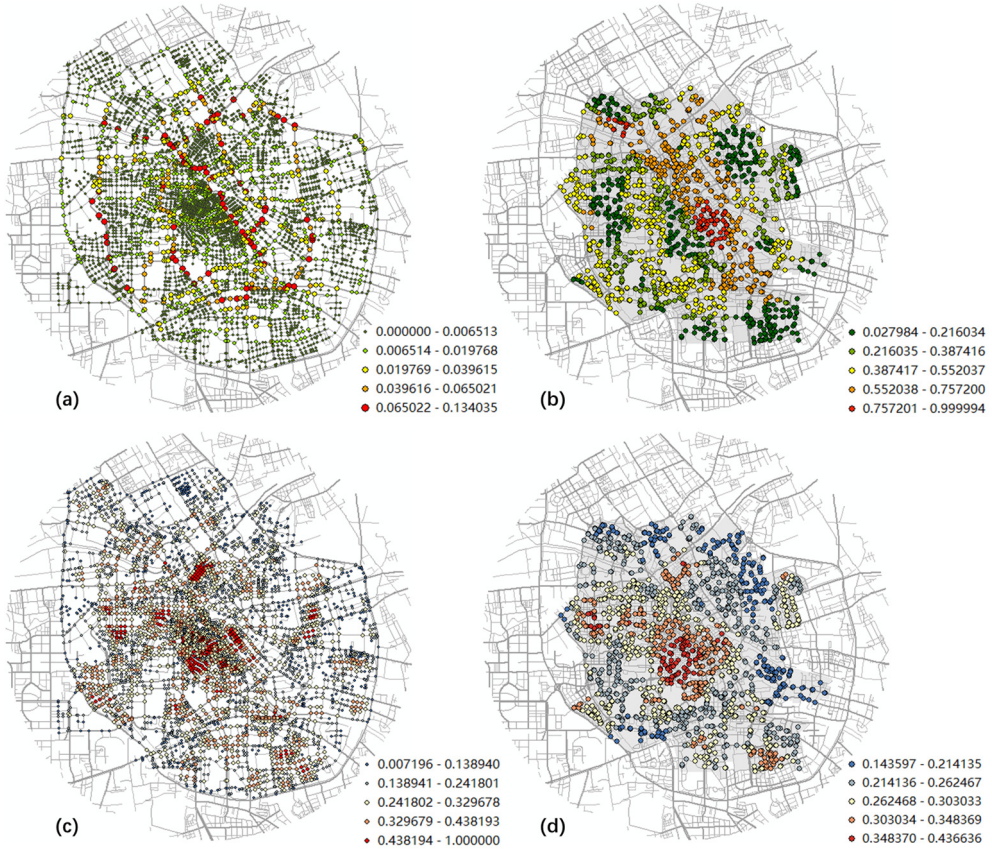


**Figure 6.** Color-coded maps representing the spatial distributions of node and network centrality. (**a**,**b**) separately present the node and network betweenness centrality while (**c**,**d**) show that of eigenvector centrality.

#### 4.2.2. Major Morphometric-Based Street Patterns

Major morphometric-based street patterns were derived according to the hierarchical clustering result. Figure 7 demonstrates that the silhouette score converged with the increase in the number of clusters in the calculation results of the three distance functions. In general, fewer clusters may successfully capture more general differences between various patterns for straightforward interpretation. However, if the number is too small, it will bypass the main differences. Conversely, a larger number will reveal more subtle differences, while at the same time, it will increase the complexity and similarity of the classification results. In this study, the number of clusters was determined as four, and the complete linkage was taken as the distance function.

The distributions of street patterns are shown in Figure 8, with Table 3 providing metrics and simplified network diagrams for each type. Street patterns of the same type tended to be spatially clustered, which is reasonable due to the continuity of the road network, with types 1 and 3 being more concentrated in the city center. By visually examining Table 3, type 1 was particularly distinguishable by its 'tree-like' network structures that are affiliated with a major road. Types 2 and 3 had clear identities as the gridiron and parallel typologies, while type 4 appeared more complicated and hybrid. Combining different metric parameters of four types and earlier predefined street patterns, the categorized street patterns were identified.

(1) Type 1 was identified as the 'dense loops on a stick', reflected in the highest betweenness centrality of 0.740. It is a street pattern with smaller blocks affiliated with the artillery road, considering the relatively high value of road density and number of intersections. This type of catchment area is mainly distributed linearly along the banks

of the river in the old city center, where many dense road networks form T-junctions with the main roads.

(2) Type 2 was the 'sparse grid', as it had the lowest value of all the metrics. Most street junctions in each catchment link four similar roads, connected throughout the network. It is widely distributed in large-scale blocks on the edge of the inner city.

(3) Type 3, 'dense gridiron and parallel', is a typical pattern that distinguishes itself from the others with the highest road density and a relatively low centrality. Mostly located in the old city center, it tends to have a nonhierarchical network structure and, thus, provide relatively better connectivity.

(4) Type 4 was the 'sparse mixed network', which falls between types 1 and 2. Although it shows a certain degree of regularity and uniformity compared to type 1, it is way less rigid than type 2. This was reflected in the medium average centrality of 0.564, average road density of 6.410, and average intersection number of 48.137.

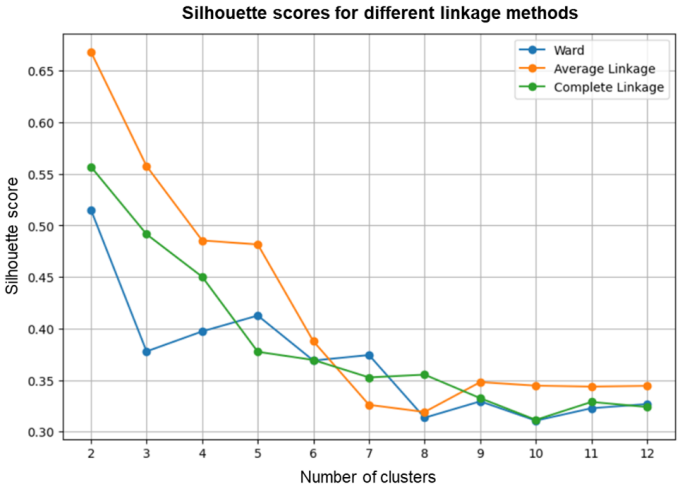


**Figure 7.** Silhouette score for clustering.

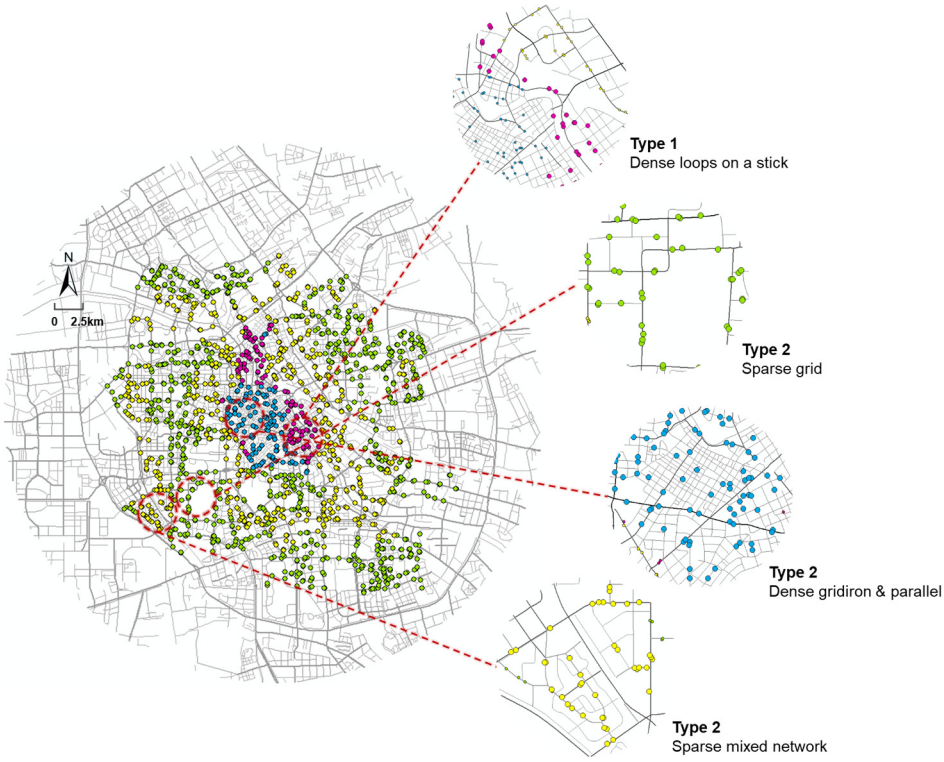


**Figure 8.** The mapping of morphometric-based street patterns in Tianjin.

**Table 3.** Definition and descriptive analysis of the variables (N = 1719).

| Types | Cluster Counts | Metrix | Betweenness Centrality | Road Density | Number of Intersections | Simplified Road Network Diagram |
|---|---|---|---|---|---|---|
| 1. Dense loops on a stick | 116 | Mean | 0.740 | 9.596 | 104.612 |  |
| | | MSS | 0.583 | 93.220 | 11,518.284 | |
| 2. Sparse grid | 867 | Mean | 0.248 | 5.771 | 42.131 | 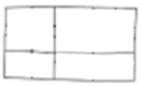 |
| | | MSS | 0.078 | 34.477 | 1938.602 | |
| 3. Dense gridiron and parallel | 129 | Mean | 0.318 | 11.661 | 158.457 |  |
| | | MSS | 0.132 | 139.796 | 28,274.752 | |
| 4. Sparse mixed network | 607 | Mean | 0.564 | 6.410 | 48.137 |  |
| | | MSS | 0.328 | 42.111 | 2509.517 | |

In general, the morphometric-based street patterns captured the differences between patterns from different perspectives. There was a certain degree of fit with the conventional patterns. According to the particularity of cycling behavior, indicators reflecting the scale of the block were also considered. In terms of the spatial distribution of clusters, it had a high coupling degree with the spatial hotspots of DBS–bus integration usage.

In addition, we also deciphered the inverse cumulative distribution probability of points and network betweenness centralities in different clusters (Figure 9), so as to supplement more comprehensive information for street patterns [57]. Figure 9a shows the two types of centralities of all bus stop catchment areas. For a better display, the point centrality was normalized. Interestingly, the cumulative distributions of dense and sparse patterns had high similarities, respectively, so we also combined the results of categories 1 and 3 and categories 2 and 4 according to the block scale. As can be seen from Figure 9b,c, the point centrality within the catchment area of all clusters exhibited a broad-scale distribution, accompanied by a truncated power-law distribution. The lower the centrality of the cluster, such as types 2 and 3, the more likely it is to have a heavy-tailed distribution. For network centrality, the frequencies of low and high values were higher in the two dense categories, showing an obvious polarization phenomenon (Figure 9d). Nevertheless, the frequency distribution of centrality in types 2 and 4 was relatively even (Figure 9e). This indicated that a grid-like road network has a higher proportion of high-connectivity intersections. Moreover, in smaller communities, the road hierarchy structure changed more dramatically within the same cycling range than in bigger communities.

### *4.3. Influence of Road Features on DBS–Bus Integration*

Before applying the zero-inflated negative binomial (ZINB) model, the distribution of the data was assessed. Tests confirmed a significant variance greater than the mean, validating the use of a negative binomial distribution. Additionally, the presence of excess zero values was established, supporting the application of the ZINB model. Tables 4–6 outline the model results for DBS–bus integration across different scenarios and time periods. In the models, the density of Points of Interest (POIs) was used as an inflation variable, significantly impacting the zero counts across the nine dependent variables.

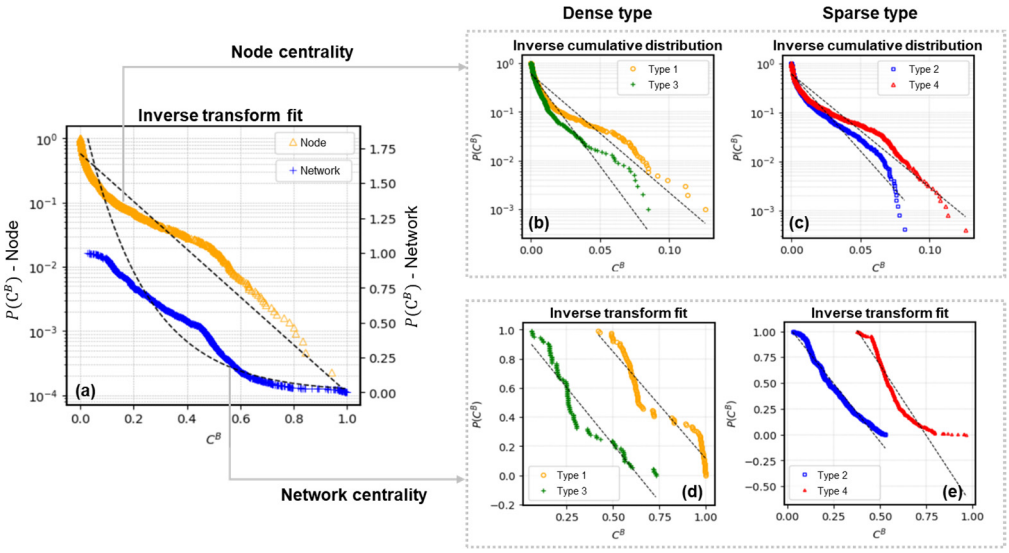


**Figure 9.** Cumulative distributions of node and network betweenness centrality in four street patterns. (**a**) includes the two types of centralities of all bus stop catchment areas. (**b**,**c**) shows the cumulative distribution of node centrality separately in dense type street patterns and sparse type, while that of network centrality are shown in (**d**,**e**).

#### 4.3.1. Different Effects on DBS–Bus Total Integrated Use during Three Time Periods

The model results for counting variables and inflation variables showed noticeable differences across three periods. As indicated in Tables 4–6, variables related to the size of road features had the most significant impact during peak hours of the week, compared with off-peak hours on weekdays and weekends. Conversely, their impact was weakest on weekends. The grade of the road where the bus stop is located was treated as an unordered categorical variable, with results presented using dummy variables. Specifically, stations located along major roads served as the reference group, where a positive coefficient suggested that this type was more likely to increase the value of the dependent variable compared to the reference group, and a negative coefficient indicated the opposite. During peak hours, bus stops along major roads clearly had the weakest attraction effect on DBS–bus integrated usage. On weekends, only stations on secondary roads showed significant positive coefficients. Similarly, the greater the density of main roads in the catchment area, the lower the frequency of integration. However, the density of the secondary roads and branches was positively correlated, except that the coefficient of branch road density was not significant on weekends. This aligns with existing research, which confirmed the negative impact of high-grade roads on cycling behavior [11,47].

For the road network structure feature variable, the higher the network betweenness centrality, the lower the frequency of total integrated usage. This suggests that significant differences in the connectivity importance of road nodes within a catchment area make it less favorable to transfer to public transport by cycling. In essence, people prefer to use bike-sharing integration in the road networks that exhibit even traffic flow. A significant negative correlation was also observed for eigenvector centrality during off-peak hours on weekdays and weekends. This may be due to some DBS use being displaced, as individuals opt for other integration options, such as walking, within more connected grid-like road networks. However, this negative effect was not evident during peak hours when travel efficiency was prioritized.

Regarding intersections, the results indicated that the number and proportion of culs-de-sac within the catchment had a significant impact at all times. In particular, the increasing of its proportion would greatly reduce the frequency. Similarly, the proportion of three-legged intersections was also negatively correlated on weekday off-peak hours and weekends. On the one hand, this is consistent with previous research, to some extent, that verified intersections typically hinder the cycling behavior by increasing the time

delay of cycling trips with traffic lights equipped at street corners [17,58,59]. On the other hand, it extends the conclusion to multi-model intersections. The negative effect of culs-de-sac usually tends to be greater than that of three-legged intersections according to their coefficients' performance.

Moreover, for the categorized street pattern, all other types had a positive effect on the DBS–bus integration frequency compared with the dense loops on a stick type. This may be due to the large traffic volume of the main road, and several three-legged intersections on the low-grade roads leading to the main road, which make cycling in the area more difficult and uncomfortable. Among these, the coefficient was higher in the two sparse street patterns. This indicated that the larger block scale is somewhat unfriendly to walking, thereby encouraging more cycling integration behavior. In dense grid-like road networks, however, there was no significant increase in the number of people choosing to ride bikes, especially during periods when travel was less urgent.

The farther a bus stop is from the nearest metro station, the more frequent the integration will be. This reflects the competitive relationship between buses and subways for passenger flow. When they are sparsely distributed, the public travel needs of individuals moving around the bus stations mainly rely on the transportation system, thus increasing the frequency of DBS–bus integration. In contrast, this phenomenon is more pronounced during the week. This may be because, during the week, people are subject to travel time constraints and the acceptable public transport connection radius is shorter, while on weekends they may have more time to travel directly by subway. Distance to the CBD and the transfer distance both showed an obvious negative correlation in all three periods. That is, catchment areas on the edge of the inner city, and stations with a longer average riding distance to reach based on usage habits, had a lower frequency of integration use.

The inflation variable coefficient in the ZINB model results explained the relationship between the factors and the probability of the observed value being zero. Although it did not directly present the impact of road characteristics on the frequency of integration use, it was consistent and reasonable with other conclusions. The coefficient for the number of companies and restaurants was positive, meaning that as the number of these POIs in the catchment area increased, the likelihood of a zero-integration frequency in bike-sharing also increased. This reflects the abundance of public transport options or pedestrian-friendly urban spaces in office and leisure areas. Conversely, the coefficients for residential and educational facilities were negative, indicating that individuals are more inclined to use bicycles between bus stops and areas where they live or go to school. The positive coefficient became significant around intensive shopping POIs on weekends.

#### 4.3.2. Different Effects on DBS–Bus Access Integrated Use and Egress Integrated Use

In this study, the integration behavior between bike-sharing and bus services was divided into access integration and egress integration, according to actual use scenarios. That is, the ride ends and starts within the catchment area of the bus station, respectively. Combined with three time periods, this formed the original data of six groups of situations, which were then used as dependent variables in the model calculation. This method is beneficial for uncovering the special laws governing DBS–bus integration more deeply. Since the coefficient performance of the two was consistent with the total integrated usage, the general conclusions explained above will not be repeated.

During the rush hours over the week, there were certain similarities and differences in the impact of road size characteristics on the two dependent variables. Bus stops located on residential roads experienced more access integration than those on main roads. For egress integrations, this phenomenon was more noticeable on secondary roads and residential roads. This indicated that people are more likely to cycle during peak hours when traveling to catch buses on lower-grade roads. On weekends, however, travel modes were more diverse and less constrained, and the impact of road grade was diminished. During the week, the density coefficients of main roads and secondary roads were significantly negatively and positively correlated, respectively. However, during peak hours, if the

density of branch roads around the bus station was relatively high, people's willingness to ride was relatively reduced. This may be due to the limitation of travel time, as the lower the grade of the branch road, the slower the speed, the more complicated the streets, and the lower the riding efficiency. Similarly, increases in main road density did not significantly reduce access integrated frequency on weekends.

The impact of road network structural characteristics on access integration changed greatly in different time periods, while the impact on egress integration was relatively stable. Primarily, the centrality of the road network almost did not affect people's decision whether to ride to the bus stop. However, the integration preference had more to do with the situation departing from the bus station. This means that the demand for dockless bike-sharing integration in a bus catchment area was closely related to its surrounding road topological structure. If the road connectivity around the bus stop is poor or the hierarchical structure is simple, people are more willing to cycle to their destination after getting off at the bus stop. In addition, the number and proportion of three-way intersections had no significant impact on access integration during the week, but an increase in the proportion reduced the frequency of cycling away from the bus stop. For categorized street patterns, the model results for weekday off-peak hours and weekend were very similar. During peak hours, the frequency of access integration in the other three types of street networks was significantly higher than that of dense loops on a stick. However, the difference in the frequency of egress integration in dense gridiron and parallel types was not obvious. Overall, the behavior of riding into the bus stop was more sensitive to the differences in road structure characteristics than riding out.

The regression results of two sets of variables related to transportation facilities were relatively similar. Among them, the distance from the nearest subway station positively affected the frequency of entering the bus stops in all scenarios, but it only had a significant impact on egress integration during off-peak hours on weekdays. This verified that the access integration frequency better reflected the competitive characteristics of the subway and buses in terms of travel flow than egress integration did. Furthermore, both the distance from the CBD and the transfer distance were negatively related to the dependent variables. The frequency of DBS–bus integration within the catchment area of a bus stop on the edge of the inner city was less than that in the city center.

**Table 4.** Modeling results of ZINB analysis for total integrated use, egress integrated use, and access integrated use (weekday peak hours).

| Variable | | Access Integrated Use during Weekday Peak Hours | | | Egress Integrated Use during Weekday Peak Hours | | | Total Integrated Use during Weekday Peak Hours | | |
|---|---|---|---|---|---|---|---|---|---|---|
| | | Coef. | Std. | *p* | Coef. | Std. | *p* | Coef. | Std. | *p* |
| **Count** | | | | | | | | | | |
| **Road features in size** | | | | | | | | | | |
| Road grade | Secondary road | 0.140 | 0.101 | 0.165 | 0.247 | 0.102 | 0.015 | 0.202 | 0.100 | 0.043 |
| | Branch road | 0.239 | 0.111 | 0.031 | 0.144 | 0.112 | 0.199 | 0.188 | 0.109 | 0.085 |
| | Residential road | 0.240 | 0.142 | 0.091 | 0.329 | 0.140 | 0.019 | 0.273 | 0.139 | 0.050 |
| Major road density | | −0.300 | 0.112 | 0.007 | −0.196 | 0.111 | 0.077 | −0.285 | 0.110 | 0.009 |
| Secondary road density | | 0.251 | 0.087 | 0.004 | 0.269 | 0.085 | 0.002 | 0.283 | 0.085 | 0.001 |
| Branch road density | | 0.120 | 0.050 | 0.015 | 0.079 | 0.048 | 0.101 | 0.105 | 0.048 | 0.028 |
| **Road network structure features** | | | | | | | | | | |
| Betweenness centrality | | −0.536 | 0.334 | 0.108 | −0.895 | 0.329 | 0.006 | −0.608 | 0.328 | 0.063 |
| Eigenvector centrality | | −0.021 | 3.029 | 0.994 | −9.173 | 3.033 | 0.002 | −3.584 | 2.998 | 0.232 |
| Number of 3-legged intersections | | 0.007 | 0.005 | 0.128 | 0.000 | 0.005 | 0.951 | 0.004 | 0.005 | 0.412 |
| Proportion of 3-legged intersections | | −0.275 | 1.199 | 0.819 | −2.840 | 1.215 | 0.019 | −1.298 | 1.184 | 0.273 |
| Number of culs-de-sac | | 0.136 | 0.044 | 0.002 | 0.184 | 0.043 | 0.000 | 0.161 | 0.043 | 0.000 |
| Proportion of culs-de-sac | | −2.769 | 2.532 | 0.274 | −11.212 | 2.509 | 0.000 | −6.907 | 2.447 | 0.005 |
| Categorized street pattern | Type 2 | 0.908 | 0.275 | 0.001 | 0.518 | 0.272 | 0.057 | 0.750 | 0.271 | 0.006 |
| | Type 3 | 0.458 | 0.285 | 0.108 | 0.383 | 0.281 | 0.172 | 0.459 | 0.282 | 0.103 |
| | Type 4 | 0.948 | 0.218 | 0.000 | 0.659 | 0.213 | 0.002 | 0.824 | 0.214 | 0.000 |

**Table 4.** *Cont.*

| Variable | | Access Integrated Use during Weekday Peak Hours | | | Egress Integrated Use during Weekday Peak Hours | | | Total Integrated Use during Weekday Peak Hours | | |
|---|---|---|---|---|---|---|---|---|---|---|
| | | **Coef.** | **Std.** | ***p*** | **Coef.** | **Std.** | ***p*** | **Coef.** | **Std.** | ***p*** |
| **Transport facilities** | | | | | | | | | | |
| Distance to nearby metro station | | 0.290 | 0.114 | 0.011 | 0.088 | 0.113 | 0.437 | 0.232 | 0.113 | 0.041 |
| Distance to CBD | | −0.266 | 0.030 | 0.000 | −0.292 | 0.030 | 0.000 | −0.282 | 0.029 | 0.000 |
| Transfer distance | | −1.499 | 0.168 | 0.000 | −1.170 | 0.200 | 0.000 | −0.852 | 0.102 | 0.000 |
| _cons | | 3.234 | 1.721 | 0.060 | 7.885 | 1.795 | 0.000 | 6.328 | 1.714 | 0.000 |
| **Inflate** | | | | | | | | | | |
| Residential use density | | −0.071 | 0.026 | 0.007 | −0.020 | 0.014 | 0.138 | −0.019 | 0.018 | 0.304 |
| Company density | | 1.900 | 0.643 | 0.003 | 1.459 | 0.803 | 0.069 | 1.623 | 1.134 | 0.152 |
| Education facility density | | −0.165 | 0.055 | 0.003 | −0.425 | 0.211 | 0.044 | −0.521 | 0.325 | 0.109 |
| Restaurant density | | 0.041 | 0.015 | 0.006 | 0.018 | 0.013 | 0.153 | 0.019 | 0.017 | 0.251 |
| Shopping use density | | 0.039 | 0.027 | 0.155 | 0.052 | 0.041 | 0.199 | 0.057 | 0.056 | 0.304 |
| _cons | | 0.873 | 1.951 | 0.655 | 1.098 | 2.792 | 0.694 | 1.383 | 2.824 | 0.624 |
| | Log-likelihood | | −5597.734 | | | −5761.958 | | | −6780.83 | |
| | LR chi2 | | 254.38 | | | 223.33 | | | 250.66 | |

**Table 5.** Modeling results of ZINB analysis for total integrated use, egress integrated use, and access integrated use (weekday off-peak hours).

| Variable | | Access Integrated Use during Weekday Off-Peak Hours | | | Egress Integrated Use during Weekday Off-Peak Hours | | | Total Integrated Use during Weekday Off-Peak Hours | | |
|---|---|---|---|---|---|---|---|---|---|---|
| | | **Coef.** | **Std.** | ***p*** | **Coef.** | **Std.** | ***p*** | **Coef.** | **Std.** | ***p*** |
| **Count** | | | | | | | | | | |
| **Road features in size** | | | | | | | | | | |
| Road grade | Secondary road | 0.092 | 0.095 | 0.334 | 0.245 | 0.097 | 0.012 | 0.178 | 0.096 | 0.063 |
| | Branch road | 0.162 | 0.105 | 0.125 | 0.146 | 0.106 | 0.170 | 0.169 | 0.105 | 0.107 |
| | Residential road | 0.263 | 0.136 | 0.052 | 0.280 | 0.137 | 0.040 | 0.278 | 0.136 | 0.041 |
| Major road density | | −0.272 | 0.105 | 0.010 | −0.233 | 0.107 | 0.030 | −0.274 | 0.106 | 0.009 |
| Secondary road density | | 0.273 | 0.082 | 0.001 | 0.293 | 0.081 | 0.000 | 0.297 | 0.081 | 0.000 |
| Branch road density | | 0.117 | 0.047 | 0.013 | 0.084 | 0.049 | 0.083 | 0.114 | 0.047 | 0.016 |
| **Road network structure features** | | | | | | | | | | |
| Betweenness centrality | | −0.486 | 0.312 | 0.119 | −0.715 | 0.315 | 0.023 | −0.540 | 0.313 | 0.085 |
| Eigenvector centrality | | −3.391 | 2.770 | 0.221 | −9.411 | 2.932 | 0.001 | −6.244 | 2.840 | 0.028 |
| Number of 3-legged intersections | | 0.002 | 0.004 | 0.623 | 0.007 | 0.005 | 0.128 | 0.005 | 0.004 | 0.314 |
| Proportion of 3-legged intersections | | −1.659 | 1.107 | 0.134 | −3.556 | 1.166 | 0.002 | −2.615 | 1.130 | 0.021 |
| Number of culs-de-sac | | 0.190 | 0.041 | 0.000 | 0.125 | 0.043 | 0.003 | 0.154 | 0.042 | 0.000 |
| Proportion of culs-de-sac | | −6.705 | 2.401 | 0.005 | −7.220 | 2.472 | 0.003 | −6.883 | 2.406 | 0.004 |
| Categorized street pattern | Type 2 | 0.786 | 0.248 | 0.002 | 0.488 | 0.251 | 0.052 | 0.636 | 0.248 | 0.010 |
| | Type 3 | 0.429 | 0.262 | 0.102 | 0.302 | 0.266 | 0.256 | 0.396 | 0.264 | 0.133 |
| | Type 4 | 0.782 | 0.197 | 0.000 | 0.498 | 0.196 | 0.011 | 0.642 | 0.196 | 0.001 |
| **Transport facilities** | | | | | | | | | | |
| Distance to nearby metro station | | 0.220 | 0.105 | 0.037 | 0.132 | 0.104 | 0.206 | 0.183 | 0.105 | 0.082 |
| Distance to CBD | | −0.275 | 0.028 | 0.000 | −0.279 | 0.029 | 0.000 | −0.276 | 0.028 | 0.000 |
| Transfer distance | | −1.568 | 0.188 | 0.000 | −1.288 | 0.218 | 0.000 | −0.829 | 0.110 | 0.000 |
| _cons | | 5.582 | 1.625 | 0.001 | 8.227 | 1.737 | 0.000 | 7.854 | 1.665 | 0.000 |
| **Inflate** | | | | | | | | | | |
| Residential use density | | −0.037 | 0.021 | 0.081 | −0.111 | 0.079 | 0.159 | −0.025 | 0.011 | 0.027 |
| Company density | | 0.956 | 0.380 | 0.012 | 3.001 | 1.625 | 0.065 | 0.708 | 0.273 | 0.010 |
| Education facility density | | −0.105 | 0.050 | 0.036 | −0.244 | 0.118 | 0.039 | −0.097 | 0.041 | 0.019 |
| Restaurant density | | 0.020 | 0.012 | 0.091 | −0.025 | 0.027 | 0.354 | 0.011 | 0.006 | 0.095 |
| Shopping use density | | 0.017 | 0.019 | 0.366 | 0.015 | 0.009 | 0.037 | 0.013 | 0.014 | 0.355 |
| _cons | | 0.761 | 1.316 | 0.563 | 6.750 | 4.255 | 0.113 | 0.839 | 0.964 | 0.384 |
| | Log-likelihood | | 6168.248 | | | −6220.705 | | | −7308.395 | |
| | LR chi2 | | 248.93 | | | 231.64 | | | 259.45 | |

**Table 6.** Modeling results of ZINB analysis for total integrated use, egress integrated use, and access integrated use (weekend).

| Variable | | Access Integrated Use during Weekend | | | Egress Integrated use During Weekend | | | Total Integrated Use during Weekend | | |
|---|---|---|---|---|---|---|---|---|---|---|
| | | Coef. | Std. | *p* | Coef. | Std. | *p* | Coef. | Std. | *p* |
| **Count** | | | | | | | | | | |
| **Road features in size** | | | | | | | | | | |
| Road grade | Secondary road | 0.137 | 0.101 | 0.177 | 0.244 | 0.100 | 0.015 | 0.178 | 0.099 | 0.073 |
| | Branch road | 0.103 | 0.113 | 0.364 | 0.075 | 0.112 | 0.504 | 0.084 | 0.110 | 0.449 |
| | Residential road | 0.201 | 0.146 | 0.169 | 0.187 | 0.145 | 0.198 | 0.174 | 0.144 | 0.227 |
| Major road density | | −0.171 | 0.110 | 0.119 | −0.212 | 0.110 | 0.054 | −0.197 | 0.108 | 0.068 |
| Secondary road density | | 0.248 | 0.087 | 0.004 | 0.250 | 0.086 | 0.003 | 0.250 | 0.085 | 0.003 |
| Branch road density | | 0.076 | 0.050 | 0.125 | 0.029 | 0.049 | 0.559 | 0.056 | 0.049 | 0.244 |
| **Road network structure features** | | | | | | | | | | |
| Betweenness centrality | | −0.476 | 0.332 | 0.151 | −0.985 | 0.332 | 0.003 | −0.712 | 0.322 | 0.027 |
| Eigenvector centrality | | −5.351 | 2.941 | 0.069 | −8.983 | 2.982 | 0.003 | −6.815 | 2.907 | 0.019 |
| Number of 3-legged intersections | | 0.002 | 0.005 | 0.636 | 0.006 | 0.005 | 0.229 | 0.004 | 0.005 | 0.355 |
| Proportion of 3-legged intersections | | −2.035 | 1.201 | 0.090 | −3.590 | 1.214 | 0.003 | −2.744 | 1.180 | 0.020 |
| Number of culs-de-sac | | 0.213 | 0.044 | 0.000 | 0.180 | 0.045 | 0.000 | 0.196 | 0.044 | 0.000 |
| Proportion of culs-de-sac | | −8.254 | 2.615 | 0.002 | −9.716 | 2.637 | 0.000 | −8.819 | 2.576 | 0.001 |
| Categorized street pattern | Type 2 | 0.635 | 0.253 | 0.012 | 0.487 | 0.256 | 0.057 | 0.555 | 0.250 | 0.027 |
| | Type 3 | 0.343 | 0.275 | 0.213 | 0.203 | 0.272 | 0.455 | 0.275 | 0.269 | 0.308 |
| | Type 4 | 0.657 | 0.203 | 0.001 | 0.554 | 0.202 | 0.006 | 0.598 | 0.200 | 0.003 |
| **Transport facilities** | | | | | | | | | | |
| Distance to nearby metro station | | 0.210 | 0.115 | 0.069 | 0.051 | 0.109 | 0.639 | 0.138 | 0.110 | 0.209 |
| Distance to CBD | | −0.256 | 0.031 | 0.000 | −0.245 | 0.031 | 0.000 | −0.255 | 0.030 | 0.000 |
| Transfer distance | | −1.199 | 0.206 | 0.000 | −1.016 | 0.231 | 0.000 | −0.670 | 0.118 | 0.000 |
| _cons | | 6.190 | 1.730 | 0.000 | 8.334 | 1.820 | 0.000 | 8.189 | 1.728 | 0.000 |
| **Inflate** | | | | | | | | | | |
| Residential use density | | −0.013 | 0.007 | 0.058 | −0.020 | 0.008 | 0.015 | −0.014 | 0.006 | 0.014 |
| Company density | | 0.560 | 0.256 | 0.029 | 0.827 | 0.246 | 0.001 | 0.606 | 0.205 | 0.003 |
| Education facility density | | −0.140 | 0.069 | 0.044 | −0.165 | 0.054 | 0.002 | −0.152 | 0.057 | 0.008 |
| Restaurant density | | 0.009 | 0.004 | 0.029 | 0.010 | 0.005 | 0.028 | 0.008 | 0.004 | 0.032 |
| Shopping use density | | 0.011 | 0.014 | 0.434 | 0.023 | 0.012 | 0.053 | 0.019 | 0.010 | 0.072 |
| _cons | | 1.660 | 0.999 | 0.097 | 1.684 | 1.009 | 0.095 | 1.528 | 0.908 | 0.092 |
| | Log-likelihood | | 5267.699 | | | −5324.785 | | | −6383.54 | |
| | LR chi2 | | 202.90 | | | 189.20 | | | 218.27 | |

## 5. Conclusions

As a convenient and efficient feeder mode for public transportation, bike-sharing is being embraced across the world. With the potential to improve the benign operation of the transportation system by reducing the environmental impact, relieving congestion, and being physically friendly to public health, DBS–bus integration could be a promising path to achieve sustainable urban transport [15]. Beyond previous studies on the impact of the urban built environment on the integration of DBS and buses, this study contributed to the bike-sharing literature by exploring the influence of urban road characteristics on DBS–bus integration. Attention was paid to the multi-scenario integration usage of around 1719 bus stops in the inner city of Tianjin. The ZINB model was also applied to analyze the specific influence of road size and network structure characteristics more accurately. The key findings are summarized as follows:

(1) The peak hours of access integration and egress integration on weekends were longer than those on weekdays, but the frequency was only two-thirds of that on weekdays. During the week, there was a significant noon peak in transfer cycling. The average transfer distance and time of DBS–bus integration were about 1690 m and 900 s, and the values were higher between 10:00 AM and 11:00 AM and after 4:00 PM. It also showed the key role of efficient DBS–bus integration in suburban–downtown commuting and movement for leisure and entertainment on weekends.

(2) Based on hierarchical clustering of network betweenness centrality, the number of intersections, and road density, the urban street network within the catchment area of bus stops was divided into four types: dense loops on a stick, sparse grid, dense gridiron and parallel, and sparse mixed network. This not only fit the conventional

predefined patterns to a certain extent, but also took the block scale into account. The spatial distribution of the clustering results was highly coupled with the spatial hotspots of DBS–bus integrated usage.

(3) High-grade roads had a negative impact on cycling behavior, and this impact was more obvious on weekdays than on weekends. Especially in the morning and evening rush hours, people were more inclined to ride bikes when taking buses on lower-grade roads, such as a branch road instead of a major road. For the road structure, there were more bike-sharing connections in the road networks with uniform grade. The increase in the proportion of three-legged intersections and culs-de-sac in the catchment makes riding more difficult, thus reducing the willingness of DBS–bus integration.

(4) The effects of road network characteristics on the DBS–bus integration differed between access integration and egress integration. The increase in the density of major roads reduced the frequency of egress integration, but the impact on access integration on weekends was not obvious. The behavior of riding into the bus stop was more sensitive to the difference in road structure characteristics than riding out. In addition, the frequency of access integration could better reflect the passenger flow competition between the subway and the bus.

The in-depth discussion of the relationship between DBS–bus integration and urban road attributes is likely to be conducive to the encouragement and management of public transportation. The above findings have important policy and operational significance for governments, operators, and citizens. For bike-sharing operators, it is indispensable to identify the hotspot regions and periods of different transfer and riding behaviors to guide the real-time relocation of bike-sharing resources. For example, the deployment at bus stations farther away from subway stations on weekdays should be increased, and on weekends, more attention should be paid to increasing the deployment at bus stations around residential areas on the edge of the inner city. Additionally, it should be allocated according to the number and proportion of surrounding service facilities to improve the possibility of bike-sharing to be chosen as a transfer mode. However, the disorderly parking problem of shared bikes in many Chinese cities is still very serious at present [60], which should be managed according to the regional and time characteristics of cycling behavior. The government's role in promoting DBS–bus connection is also crucial. Since the prosperity of dockless bike-sharing in 2016, the national or local governments have promulgated a number of policies and plans, including the Tianjin Internet Rental Bicycle Management Interim Measures, enacted by the Tianjin Transport and Traffic Commission. In these policies and plans, it is called for to improve the cycling environment in areas around bus stations and along bicycle lanes to promote riding comfort and safety. Based on the findings of this paper, relevant practices should start from both road form and traffic facility planning, as well as traffic policy management. For example, focusing on the design of road sections around bus stops on high-grade roads, and isolating safe and convenient bicycle lanes through green belts. The large-scale networks of a single main road and its ancillary roads should be avoided in planning, and the balance of road network flow should be ensured, especially in linear spaces along urban rivers [61]. Specific bicycle parking areas around stations with large traffic should be set up to eliminate road obstacles [62]. Similar interventions to improve the cycling environment may be helpful to attract more DBS–bus users.

There were some limitations in this study. It could be improved in the method of measuring DBS–bus integration frequency. Due to the overlapping parking areas in the same driving direction, the catchment areas for different directions could not be distinguished, which could easily cause a little deviation from the actual transfer frequency. In addition, the classification of street patterns and their impact on DBS–bus connection could be discussed in more detail. If neighborhood-level population data and other high-precision data reflecting the economic and social attributes are available, future research could focus on the actual operation of public transport systems more specifically.

**Author Contributions:** Conceptualization, Z.Y., Y.G., M.Z. and Y.W.; Methodology, Y.G., M.Z. and Y.W.; Validation, F.T.; Formal analysis, Y.W.; Resources, Z.Y.; Data curation, M.Z., Y.W. and F.T.; Writing—original draft, M.Z.; Visualization, Z.Y.; Funding acquisition, Y.G. All authors have read and agreed to the published version of the manuscript.

**Funding:** This study was jointly supported by grants from the National Natural Science Foundation of China (No. 52308073) and Tianjin Applied Basic Research Youth Project (No. 22JCQNJC01170).

**Data Availability Statement:** The data that has been used is confidential.

**Conflicts of Interest:** The authors declare no conflict of interest.

## References

1. Yang, L.; Chau, K.W.; Szeto, W.Y.; Cui, X.; Wang, X. Accessibility to Transit, by Transit, and Property Prices: Spatially Varying Relationships. *Transp. Res. Part D-Transp. Environ.* **2020**, *85*, 102387. [CrossRef]
2. Yang, L.; Liang, Y.; He, B.; Yang, H.; Lin, D. COVID-19 Moderates the Association between To-metro and By-metro Accessibility and House Prices. *Transp. Res. Part D-Transp. Environ.* **2019**, *114*, 103571. [CrossRef]
3. Ma, T.; Knaap, G.J. Estimating the Impacts of Capital Bikeshare on Metrorail Ridership in the Washington Metropolitan Area. *Transp. Res. Rec.* **2019**, *2673*, 371–379. [CrossRef]
4. Zhou, Y.; Yu, Y.; Wang, Y.; He, B.; Yang, L. Mode Substitution and Carbon Emission Impacts of Electric Bike Sharing Systems. *Sust. Cities Soc.* **2023**, *89*, 104312. [CrossRef]
5. Cheng, L.; Huang, J.; Jin, T.; Chen, W.; Li, A.; Witlox, F. Comparison of Station-Based and Free-Floating Bikeshare Systems as Feeder Modes to the Metro. *J. Transp. Geogr.* **2023**, *107*, 103545. [CrossRef]
6. Wang, Y.; Li, J.; Yang, X.; Guo, Y.; Ren, J.; Zhan, Z. Examining the Impact of Station Location on Dockless Bikesharing-Metro Integration: Evidence from Beijing. *Travel. Behav. Soc.* **2024**, *37*, 100835. [CrossRef]
7. Zhan, Z.; Guo, Y.; Noland, R.B.; He, S.Y.; Wang, Y. Analysis of Links between Dockless Bikeshare and Metro Trips in Beijing. *Transp. Res. Part A Policy Pract.* **2023**, *175*, 103784. [CrossRef]
8. Guo, Y.; Yang, L.; Wang, W.; Guo, Y. Traffic Safety Perception, Attitude, and Feeder Mode Choice of Metro Commute: Evidence from Shenzhen. *Int. J. Environ. Res. Public Health* **2020**, *17*, 9402. [CrossRef] [PubMed]
9. Liu, Y.; Ji, Y.; Feng, T.; Shi, Z. Use Frequency of Metro-Bikeshare Integration: Evidence from Nanjing, China. *Sustainability* **2020**, *12*, 1426. [CrossRef]
10. Chen, Z.; van Lierop, D.; Ettema, D. Dockless Bike-Sharing Systems: What Are the Implications? *Transp. Rev.* **2020**, *40*, 333–353. [CrossRef]
11. Guo, Y.; He, S.Y. Built Environment Effects on the Integration of Dockless Bike-Sharing and the Metro. *Transp. Res. D Transp. Environ.* **2020**, *83*, 102335. [CrossRef]
12. Ma, X.; Ji, Y.; Yang, M.; Jin, Y.; Tan, X. Understanding Bikeshare Mode as a Feeder to Metro by Isolating Metro-Bikeshare Transfers from Smart Card Data. *Transp. Policy* **2018**, *71*, 57–69. [CrossRef]
13. Ricci, M. Bike Sharing: A Review of Evidence on Impacts and Processes of Implementation and Operation. *Res. Transp. Bus. Manag.* **2015**, *15*, 28–38. [CrossRef]
14. Tarpin-Pitre, L.; Morency, C. Typology of Bikeshare Users Combining Bikeshare and Transit. *Transp. Res. Rec.* **2020**, *2674*, 475–483. [CrossRef]
15. Guo, Y.; Yang, L.; Lu, Y.; Zhao, R. Dockless Bike-Sharing as a Feeder Mode of Metro Commute? The Role of the Feeder-Related Built Environment: Analytical Framework and Empirical Evidence. *Sustain. Cities Soc.* **2021**, *65*, 102594. [CrossRef]
16. Cheng, L.; Jin, T.; Wang, K.; Lee, Y.; Witlox, F. Promoting the Integrated Use of Bikeshare and Metro: A Focus on the Nonlinearity of Built Environment Effects. *Multimodal Transp.* **2022**, *1*, 100004. [CrossRef]
17. Guo, Y.; He, S.Y. Perceived Built Environment and Dockless Bikeshare as a Feeder Mode of Metro. *Transp. Res. Part D Transp. Environ.* **2021**, *92*, 102693. [CrossRef]
18. Zhou, X.; Dong, Q.; Huang, Z.; Yin, G.; Zhou, G.; Liu, Y. The Spatially Varying Effects of Built Environment Characteristics on the Integrated Usage of Dockless Bike-Sharing and Public Transport. *Sustain. Cities Soc.* **2023**, *89*, 104348. [CrossRef]
19. Ni, Y.; Chen, J. Exploring the Effects of the Built Environment on Two Transfer Modes for Metros: Dockless Bike Sharing and Taxis. *Sustainability* **2020**, *12*, 2034. [CrossRef]
20. Jiang, B.; Claramunt, C. Topological Analysis of Urban Street Networks. *Environ. Plan. B Plan. Des.* **2004**, *31*, 151–162. [CrossRef]
21. Gehl, J. *Life between the Buildings: Using Public Space*; The Danish Architectural Press: Copenhagen, Danmark, 1987.
22. Wu, X.; Lu, Y.; Lin, Y.; Yang, Y. Measuring the Destination Accessibility of Cycling Transfer Trips in Metro Station Areas: A Big Data Approach. *Int. J. Environ. Res. Public Health* **2019**, *16*, 2641. [CrossRef] [PubMed]
23. Chen, G.; Wei, Z. Exploring the Impacts of Built Environment on Bike-Sharing Trips on Weekends: The Case of Guangzhou. *Int. J. Sustain. Transp.* **2024**, *18*, 315–327. [CrossRef]
24. Lin, J.J.; Zhao, P.; Takada, K.; Li, S.; Yai, T.; Chen, C.H. Built Environment and Public Bike Usage for Metro Access: A Comparison of Neighborhoods in Beijing, Taipei, and Tokyo. *Transp. Res. Part D Transp. Environ.* **2018**, *63*, 209–221. [CrossRef]

25. Zhao, B.; Deng, Y.; Luo, L.; Deng, M.; Yang, X. Preferred Streets: Assessing the Impact of the Street Environment on Cycling Behaviors Using the Geographically Weighted Regression. *Transportation* **2024**, 1–27. [CrossRef]
26. Ji, S.; Heinen, E.; Wang, Y. Non-Linear Effects of Street Patterns and Land Use on the Bike-Share Usage. *Transp. Res. Part D Transp. Environ.* **2023**, *116*, 103630. [CrossRef]
27. Li, J.; Li, C.; Zhao, X.; Wang, X. Do Road Network Patterns and Points of Interest Influence Bicycle Safety? Evidence from Dockless Bike Sharing in China and Policy Implications for Traffic Safety Planning. *Transp. Policy* **2024**, *149*, 21–35. [CrossRef]
28. Buhl, J.; Gautrais, J.; Solé, R.V.; Kuntz, P.; Valverde, S.; Deneubourg, J.L.; Theraulaz, G. Efficiency and Robustness in Ant Networks of Galleries. *Eur. Phys. J. B* **2004**, *42*, 123–129. [CrossRef]
29. Jin, Y.; Wang, X.S.; Chen, X.H. Incorporating Road Network Structures into Macro Level Traffic Safety Analysis. In Proceedings of the ICCTP 2011: Towards Sustainable Transportation Systems—Proceedings of the 11th International Conference of Chinese Transportation Professionals, Nanjing, China, 14–17 August 2011.
30. Wang, X.; You, S.; Wang, L. Classifying Road Network Patterns Using Multinomial Logit Model. *J. Transp. Geogr.* **2017**, *58*, 104–112. [CrossRef]
31. Zhang, Y.; Bigham, J.; Ragland, D.; Chen, X. Investigating the Associations between Road Network Structure and Non-Motorist Accidents. *J. Transp. Geogr.* **2015**, *42*, 34–47. [CrossRef]
32. Jiang, B.; Jia, T. Agent-Based Simulation of Human Movement Shaped by the Underlying Street Structure. *Int. J. Geogr. Inf. Sci.* **2011**, *25*, 51–64. [CrossRef]
33. Pasha, M.; Rifaat, S.; Tay, R.; de Barros, A. Urban Design and Planning Influences on the Share of Trips Taken by Cycling. *J. Urban. Des.* **2016**, *21*, 471–480. [CrossRef]
34. Lee, J.; Choi, K.; Leem, Y. Bicycle-Based Transit-Oriented Development as an Alternative to Overcome the Criticisms of the Conventional Transit-Oriented Development. *Int. J. Sustain. Transp.* **2016**, *10*. [CrossRef]
35. Luo, S.; Nie, Y. Integrated Design of a Bus-Bike System Considering Realistic Route Options and Bike Availability. *Transp. Res. Part C Emerg. Technol.* **2023**, *153*, 975–984. [CrossRef]
36. Ji, Y.; Fan, Y.; Ermagun, A.; Cao, X.; Wang, W.; Das, K. Public Bicycle as a Feeder Mode to Rail Transit in China: The Role of Gender, Age, Income, Trip Purpose, and Bicycle Theft Experience. *Int. J. Sustain. Transp.* **2017**, *11*, 308–317. [CrossRef]
37. Chen, Z.; van Lierop, D.; Ettema, D. Exploring Dockless Bikeshare Usage: A Case Study of Beijing, China. *Sustainability* **2020**, *12*, 1238. [CrossRef]
38. Chan, K.; Farber, S. Factors Underlying the Connections between Active Transportation and Public Transit at Commuter Rail in the Greater Toronto and Hamilton Area. *Transportation* **2020**, *47*, 2157–2178. [CrossRef]
39. Weliwitiya, H.; Rose, G.; Johnson, M. Bicycle Train Intermodality: Effects of Demography, Station Characteristics and the Built Environment. *J. Transp. Geogr.* **2019**, *74*, 395–404. [CrossRef]
40. Campbell, K.B.; Brakewood, C. Sharing Riders: How Bikesharing Impacts Bus Ridership in New York City. *Transp. Res. Part A Policy Pract.* **2017**, *100*, 264–282. [CrossRef]
41. Cervero, R.; Caldwell, B.; Cuellar, J. Bike-and-Ride: Build It and They Will Come. *J. Public Trans.* **2013**, *16*, 83–105. [CrossRef]
42. Martens, K. Promoting Bike-and-Ride: The Dutch Experience. *Transp. Res. Part A Policy Pract.* **2007**, *41*, 326–338. [CrossRef]
43. Martin, E.W.; Shaheen, S.A. Evaluating Public Transit Modal Shift Dynamics in Response to Bikesharing: A Tale of Two U.S. Cities. *J. Transp. Geogr.* **2014**, *41*, 315–324. [CrossRef]
44. Liu, Y.; Ji, Y.; Feng, T.; Timmermans, H. Understanding the Determinants of Young Commuters' Metro-Bikeshare Usage Frequency Using Big Data. *Travel. Behav. Soc.* **2020**, *21*, 121–130. [CrossRef]
45. Yang, Y.; Heppenstall, A.; Turner, A.; Comber, A. A Spatiotemporal and Graph-Based Analysis of Dockless Bike Sharing Patterns to Understand Urban Flows over the Last Mile. *Comput. Environ. Urban. Syst.* **2019**, *77*, 101361. [CrossRef]
46. Porta, S.; Crucitti, P.; Latora, V. The Network Analysis of Urban Streets: A Dual Approach. *Phys. A Stat. Mech. Its Appl.* **2006**, *369*, 853–866. [CrossRef]
47. Zhang, Y.; Thomas, T.; Brussel, M.; van Maarseveen, M. Exploring the Impact of Built Environment Factors on the Use of Public Bikes at Bike Stations: Case Study in Zhongshan, China. *J. Transp. Geogr.* **2017**, *58*, 59–70. [CrossRef]
48. Zhang, Y.; Wang, X.; Zeng, P.; Chen, X. Centrality Characteristics of Road Network Patterns of Traffic Analysis Zones. *Transp. Res. Rec.* **2011**, *2256*, 16–24. [CrossRef]
49. Freeman, L.C. A Set of Measures of Centrality Based on Betweenness. *Sociometry* **1977**, *40*, 35–41. [CrossRef]
50. Wasserman, S.; Faust, K. Social Network Analysis in the Social and Behavioral Sciences. In *Social Network Analysis: Methods and Applications*; Cambridge University Press: Cambridge, UK, 2012.
51. Bonacich, P. Some Unique Properties of Eigenvector Centrality. *Soc. Netw.* **2007**, *29*, 555–564. [CrossRef]
52. Jiang, S.; Alves, A.; Rodrigues, F.; Ferreira, J.; Pereira, F.C. Mining Point-of-Interest Data from Social Networks for Urban Land Use Classification and Disaggregation. *Comput. Environ. Urban. Syst.* **2015**, *53*, 36–46. [CrossRef]
53. Liu, X.; Long, Y. Automated Identification and Characterization of Parcels with OpenStreetMap and Points of Interest. *Environ. Plan. B Plan. Des.* **2016**, *43*, 341–360. [CrossRef]
54. Yue, Y.; Zhuang, Y.; Yeh, A.G.O.; Xie, J.Y.; Ma, C.L.; Li, Q.Q. Measurements of POI-Based Mixed Use and Their Relationships with Neighbourhood Vibrancy. *Int. J. Geogr. Inf. Sci.* **2017**, *31*, 658–675. [CrossRef]

55. Desgeorges, M.M.; Nazare, J.A.; Enaux, C.; Oppert, J.M.; Menai, M.; Charreire, H.; Salze, P.; Weber, C.; Hercberg, S.; Roda, C.; et al. Perceptions of the Environment Moderate the Effects of Objectively-Measured Built Environment Attributes on Active Transport. An ACTI-Cités Study. *J. Transp. Health* **2021**, *20*, 100972. [CrossRef]
56. Lee, S.; Smart, M.J.; Golub, A. Difference in Travel Behavior between Immigrants in the U.S. and U.S. Born Residents: The Immigrant Effect for Car-Sharing, Ride-Sharing, and Bike-Sharing Services. *Transp. Res. Interdiscip. Perspect.* **2021**, *9*, 100296. [CrossRef]
57. Crucitti, P.; Latora, V.; Porta, S. Centrality Measures in Spatial Networks of Urban Streets. *Phys. Rev. E Stat. Nonlin Soft Matter Phys.* **2006**, *73*, 36125. [CrossRef]
58. Faghih-Imani, A.; Eluru, N. Incorporating the Impact of Spatio-Temporal Interactions on Bicycle Sharing System Demand: A Case Study of New York CitiBike System. *J. Transp. Geogr.* **2016**, *54*, 218–227. [CrossRef]
59. El-Assi, W.; Salah Mahmoud, M.; Nurul Habib, K. Effects of Built Environment and Weather on Bike Sharing Demand: A Station Level Analysis of Commercial Bike Sharing in Toronto. *Transportation* **2017**, *44*, 589–613. [CrossRef]
60. Lu, M.; An, K.; Hsu, S.C.; Zhu, R. Considering User Behavior in Free-Floating Bike Sharing System Design: A Data-Informed Spatial Agent-Based Model. *Sustain. Cities Soc.* **2019**, *49*, 101567. [CrossRef]
61. Zhao, X.; Guo, Y. Planning Bikeway Network for Urban Commute based on Mobile Phone Data: A Case Study of Beijing. *Travel Behav. Soc.* **2024**, *34*, 100672. [CrossRef]
62. Zhou, Z.; Li, H.; Zhang, A. Does Bike Sharing Increase House Prices? Evidence from Micro-Level Data and the Impact of COVID-19. *J. Real Estate Financ. Econ.* **2022**, 1–30. [CrossRef]


**Disclaimer/Publisher's Note:** The statements, opinions and data contained in all publications are solely those of the individual author(s) and contributor(s) and not of MDPI and/or the editor(s). MDPI and/or the editor(s) disclaim responsibility for any injury to people or property resulting from any ideas, methods, instructions or products referred to in the content.